

## Modeling hurricane-induced wetland-bay and bay-shelf sediment fluxes

Ke Liu<sup>a,\*</sup>, Qin Chen<sup>b,c</sup>, Kelin Hu<sup>c</sup>, Kehui Xu<sup>d,e</sup>, Robert R. Twilley<sup>d</sup>

<sup>a</sup> Division of Geological and Planetary Sciences, California Institute of Technology, Pasadena, CA 91125, USA

<sup>b</sup> Department of Civil and Environmental Engineering, Louisiana State University, Baton Rouge, LA 70803, USA

<sup>c</sup> Center for Computation and Technology, Louisiana State University, Baton Rouge, LA 70803, USA

<sup>d</sup> Department of Oceanography and Coastal Sciences, Louisiana State University, Baton Rouge, LA 70803, USA

<sup>e</sup> Coastal Studies Institute, Louisiana State University, Baton Rouge, LA 70803, USA



### ARTICLE INFO

#### Keywords:

Hurricanes  
Storm surge  
Waves  
Sediment redistribution  
Morphological change  
Coastal wetlands  
Modeling  
Delft3D

### ABSTRACT

Hurricanes have long been recognized as a strong forcing in shaping the coastal morphology, especially by redistributing sediments among coastal wetlands, bays and inner continental shelves. However, the contribution of hurricane-induced sediment transport to the sediment budget of a shelf – bay – wetland system has not been evaluated using a physics-based numerical model. There is a particular confusion on how sediment transport to coastal wetlands contributes to sediment accretion in wetlands and thus wetland adaptation to sea level rise. In this paper, we present a coupled modeling system for hurricane winds, storm surge, waves and sediment transport on the Louisiana coast, and use it to investigate two fundamental questions: (1) How much sediment is transported and deposited on coastal wetlands during a major hurricane event like Hurricane Gustav (2008), and (2) where is the source of the deposited sediment on the wetland soil surface. Our model successfully reproduced the measured basin-averaged sediment accretion in the Terrebonne and Barataria Basins after Gustav, and estimated that Hurricane Gustav imported approximately 27 million metric tons of sediment on wetlands in that area. The estimated deposition was mainly made up of mud suspended from the coastal bays, and the contribution of this sediment to wetland deposition was 88.7% in Terrebonne Bay and 98.2% in Barataria Bay within the tested range of sediment properties. This paper demonstrates a useful tool to help understand how sediment dynamics in the coastal zone during hurricane events play a significant role in the sediment budget of a deltaic coast.

### 1. Introduction

The Mississippi River Delta Plain (MRDP) has the largest area of coastal wetlands in the contiguous United States, which serves multiple ecosystem functions including reduction of surge and waves during extreme events, habitat for fisheries and wildlife, and a valuable economic resource for agriculture and industry. It is widely recognized that intense hurricanes play a key role in shaping the morphology of coastal wetlands by redistributing a significant amount of sediment. Sediment accretion has been observed on the marsh surface after hurricanes and storms, and these processes are significant to maintaining marsh elevation relative to sea level rise and subsidence (Morgan et al., 1958; Chamberlain, 1959; Roberts et al., 1987; Rejmánek et al., 1988; Reed, 1989; Nyman et al., 1995; Cahoon et al., 1995; Turner et al., 2006; McKee and Cherry, 2009). On the other hand, hurricanes may have negative effects by eroding the edge of marshes and expanding the existing ponds

and small lakes (McGee et al., 2006; Morton and Barras, 2011). There is a debate on the net effect of hurricanes on coastal morphodynamics. In order to understand the effects of hurricane on the large-scale sediment budget of a coastal system, it is necessary to identify the major source of sediment deposition on coastal wetlands and sediment fluxes across land and sea boundaries.

Considerable effort has been devoted to quantifying the contribution of hurricane-induced sedimentation. Turner et al. (2006) estimated that Hurricane Katrina and Rita brought in 131 million metric tons (MMT) of mineral material to the MRDP. Tweel and Turner (2012) developed a statistical model based on the sediment deposition data observed from Hurricanes Katrina (2005), Rita (2005) and Gustav (2008), and estimated that the annual deposition on the marsh surface from category 1 or higher hurricanes was 5.6 MMT. By chronostratigraphic assessment of 27 cores taken within the Breton Sound Basin, Smith et al. (2015) suggested the annual sediment accumulation caused by category 3 or higher

\* Corresponding author.

E-mail address: [keliu@caltech.edu](mailto:keliu@caltech.edu) (K. Liu).

<sup>1</sup> Formally graduate student in the Department of Civil and Environmental Engineering, Louisiana State University.

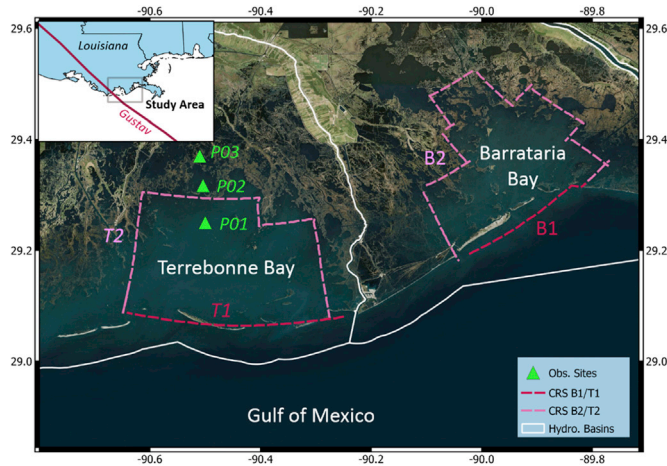


Fig. 1. Terrebonne Bay and Barataria Bay. P01/P02/P03 are the locations of model output points, T1&T2 are the cross sections in Terrebonne Bay, and B1&B2 are the cross sections in Barataria Bay.

hurricanes was only about 0.05 MMT in that area. Besides the large discrepancy between the existing estimates based on different methods, some obvious limitations exist in the above-mentioned studies: Firstly, the spatial distribution of sediment deposition in wetlands was predicted using a limited number of coring or sampling stations, and thus the effects of local bathymetry and man-made structures on sediment redistribution were not taken into account. Secondly, sediment deposition in the interior of wetlands is often associated with both local erosion and deposition, while most measurements didn't include the temporal variation of the marsh surface elevation and thus could not reproduce the erosional history of a storm event.

The source of sediment deposited in marshes during storm events includes onshore transport of marine material originating from the inner continental shelf or redistribution of local sediment in bays and estuaries of MRDP. These two sources imply different mechanisms of sediment balance and could lead to different wetland restoration strategies. A plausible hypothesis is that most deposition originates from the shallow lakes and open bays, where relatively large waves suspend sediment and the surge water moves suspended materials to the marsh surface (Chamberlain, 1959; Roberts et al., 1987; Rejmánek et al., 1988; Reed, 1989). There are few techniques available to identify the pathway of sediment transport in a typical coastal environment during an extreme event and test the dependency of these sources on sediment properties, vegetation coverage, and other local environmental factors.

Numerical models have been applied to simulate large-scale hydrodynamics, sediment transport and morphological changes for MRDP under hurricane conditions (Freeman et al., 2015; Warner et al., 2017; Xu et al., 2015; Yamashita et al., 2016). For instance, the seabed erosion and deposition on the Louisiana-Texas continental shelf after Hurricane Katrina and Rita were studied using a three-dimensional sediment

transport model based on the Regional Ocean Modeling System (ROMS) (Xu et al., 2015), and the spatial pattern of sediment accretion and erosion at Sister Lake during Hurricane Rita was simulated using MIKE21/MIKE 3 (Freeman et al., 2015). However, little has been done to model the sediment transport and morphological processes in the entire coastal system, including the continental shelf, bays, lakes, and wetlands, and to quantify the sediment exchange at shelf-bay and bay-wetland borders. In the present study, we utilize a coupled modeling system based on Delft3D, including wind, surge, waves and sediment processes for the Louisiana coast (Liu et al., 2015). We apply the model to study the short-term impact of a hurricane on sediment dynamics in coastal wetlands with the following specific objectives: (1) estimate net sediment deposition in the coastal wetlands during a major hurricane event, (2) identify the major source of deposited sediment on the wetland surface, and (3) develop sediment budgets of coastal basins as result of cyclone effects on sediment redistribution. This paper is organized as follows. The study area, model setting and measurement data are described in section 2. The modeled hydrodynamic forcing during Hurricane Gustav is validated against measurements in section 3.1. The morphodynamics and a comparison with the measured post-hurricane accretion are presented in section 3.2. The hurricane-induced sediment flux, the deposition in coastal wetlands and the sediment balance in the coastal bays are analyzed in Section 3.3 and 3.4. A discussion about the model sensitivity and uncertainty is given in section 4. A summary of our findings is presented in section 5.

2. Methods

2.1. Study area and Hurricane Gustav

Our study area is the wetland-bay-shelf system of Terrebonne and Barataria Basins in the MRDP. The Terrebonne and Barataria Basins are located in south Louisiana, between the Mississippi River and the Atchafalaya River, open to the Gulf of Mexico to the south (Fig. 1). This region encompasses 1243 square kilometers of swamp and 4221 square kilometers of marshes, grading from fresh water marsh inland to brackish and salt marshes near the bays and the gulf. Severe marsh erosion and land loss occurred in these two coastal basins from 1932 to 2010 at 1092 square kilometers in Barataria and 1191 square kilometers in Terrebonne (Couvillion et al., 2011).

This region was impacted by multiple major hurricanes in the last decade, including Katrina and Rita in 2005, Gustav and Ike in 2008 and Isaac in 2012. In this paper, we chose Hurricane Gustav as an example because the availability of a large number of field observations following this storm. Hurricane Gustav (2008) was the first major hurricane tracking through the southeast Louisiana after Katrina (2005). Although Gustav was a category 2 hurricane when it made landfall on 1 September 2008, much weaker than Katrina, its size increased as it approached the Louisiana coast. The tropical-storm-strength winds impacted this region for 12–15 h and generated significant storm surge along the Louisiana coast.

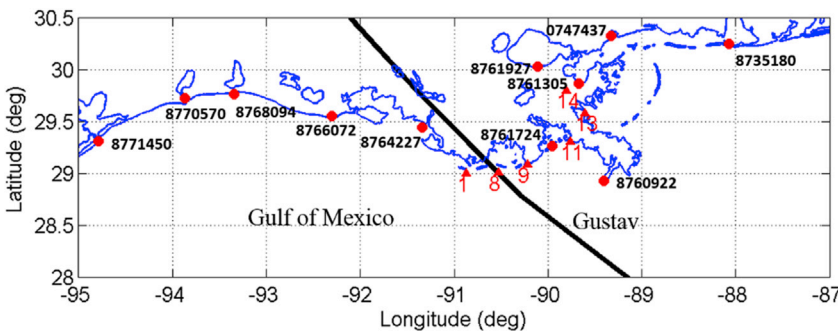


Fig. 2. The locations of NOAA tide stations (red dots) and wave gauges by Kennedy et al. (2010). (red triangles). (For interpretation of the references to color in this figure legend, the reader is referred to the Web version of this article.)

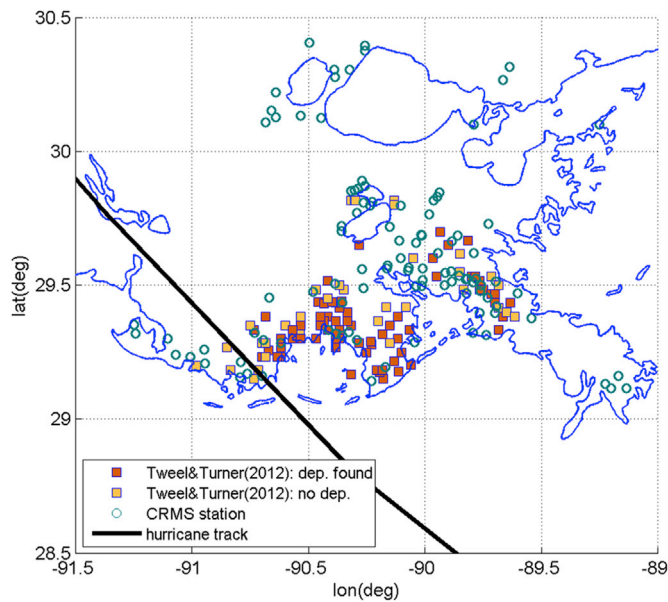


Fig. 3. The locations of the CRMS stations (circles) and the survey sites in Tweel and Turner, 2012 (rectangles).

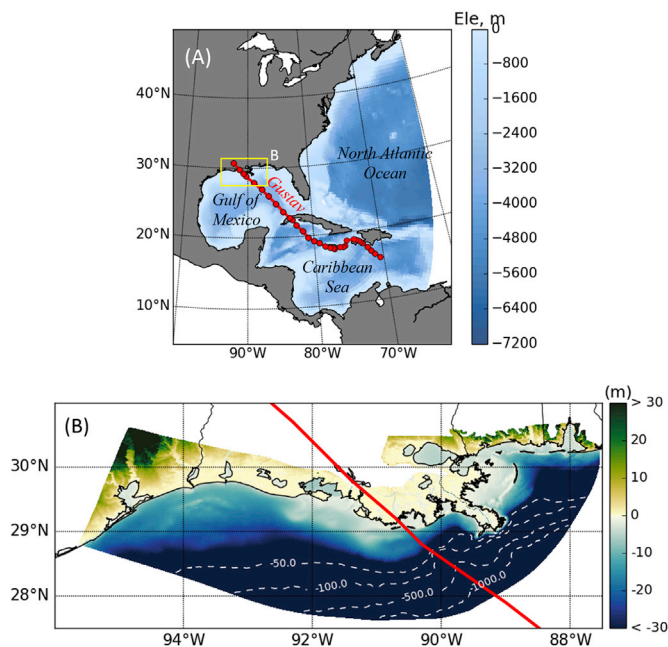


Fig. 4. Bathymetry for the nested domain. (A): Gulf of Mexico (GoM) mesh; (B): Louisiana (LA) mesh.

## 2.2. Measurement data

Several sources of measurement data were collected for model validation. These data also offer a valuable description of the evolution of storm surge and waves along the Louisiana coast and a landscape view of the sedimentation after Gustav.

### 2.2.1. National oceanic and atmospheric administration (NOAA) tidal stations

NOAA operates a national-wide network of tide stations. The measured water levels during Gustav were compared to our model results at 11 stations from Dauphin Island, Alabama, to Galveston Pleasure Pier, Texas (Fig. 2). The measured water levels are relative to mean sea level

(MSL).

### 2.2.2. Wave gauges by Kennedy et al. (2010)

Sixteen gauges deployed by Kennedy et al. (2010), provided a record of the nearshore wave behavior during Gustav. Waves and water levels were measured using bottom-mounted pressure sensors recording continuously at 1 Hz (Kennedy et al., 2010). Wave heights were computed through standard spectral methods, and surge levels were obtained by applying a low-pass filter to water levels. Among all the gauges, six of them were located within the region of our interest, and thus served as benchmarks for the modeled wave heights and wave periods (Fig. 2).

### 2.2.3. Coastwide reference monitoring system (CRMS) sites

CRMS is a joint effort by the Louisiana Coastal Protection and Restoration Authority (CPRA) and United States Geological Survey (USGS) to address the needs to monitor and evaluate the effectiveness of implemented coastal restoration projects. A total of 390 monitoring sites were operated within nine coastal basins, covering the whole Louisiana coast. Records of surge levels during Gustav within the Barataria-Terrebonne Basins were collected at 108 stations. After removing the gauges with incomplete or obviously inconsistent records near the peak of the storm, we chose the observed peak surges at 87 stations for model validation (Fig. 3).

### 2.2.4. Deposition measurement by Tweel and Turner (2012)

A field survey was conducted following the landfall of Gustav (Tweel and Turner, 2012), and the thickness of surface deposition on the coastal wetlands were measured at 110 locations in Barataria Bay, Terrebonne Bay, and a small part of Breton Sound (Fig. 3). This dataset was compared with the modeled deposition in the wetlands to calibrate our sediment transport model.

## 2.3. Model settings

### 2.3.1. Model domains

We applied the Delft3D model, which has been widely used for simulations of coastal hydrodynamic and morphodynamic processes (Horstman et al., 2015; Hu et al., 2015; Wang et al., 2017), to study the hurricane-induced sediment transport. A nested two-layer curvilinear mesh was designed to resolve the complex geometry of the Louisiana (LA) coast (Fig. 4). The Gulf of Mexico (GoM) mesh covered the Gulf of Mexico, the Caribbean Sea and part of the western North Atlantic Ocean to capture the development of the fast-moving hurricane and provide accurate surge level and current velocity to the detailed domain. The nested domain (LA mesh) extended from Galveston Bay (TX) to the west, to Mobile Bay (AL) to the east, covering the entire Louisiana coast. The GoM mesh had a grid resolution varying from 50 km in Atlantic Ocean to about 10 km near the Louisiana coast. The grid size of the LA mesh was 1–3 km on the continental shelf, 200–500 m in coastal wetlands and lakes, and 60–80 m across the Mississippi River. Although a three-dimensional model has the advantage in resolving the vertical flow structure, vegetation effects and some physical processes in sediment transport (Lapetina and Sheng, 2015), a carefully calibrated 2-D model can achieve similar accuracy in the prediction of tidal current and bed deposition at a tidal mangrove with much greater computational efficiency (Horstman et al., 2013, 2015). Moreover, the water body was probably well mixed in the inner shelf and estuaries during high-energy events such as a hurricane (Chen et al., 2008). Therefore, the 2-D version of Delft3D model was used to focus on depth-integrated sediment fluxes in the shelf-bay-wetland system and sediment mass accumulations on wetlands instead of the bottom boundary layer processes.

The bathymetric data from the SL16 mesh (Dietrich et al., 2008), which has a resolution of 4–6 km in the Gulf, 500–1000 m on the shelf, and 20–50 m in the small-scale channels and passes, was interpolated into the entire GoM mesh and a large part of the LA mesh. The digital

**Table 1**  
The physical properties and the enhanced Manning's coefficient for eleven vegetation types in the numerical model (Dietrich et al., 2008; Visser, 2007).

Vegetation type	Height (m)	Stem diameter (cm)	Density (# stems per m <sup>2</sup> )	Enhanced Manning's coefficient
Grassland	1.25	0.17	805	0.05
Cultivated	3.10	2.39	8.6	0.05
Pasture/Hay	0.32	0.50	805	0.05
Upland Forest	19.60	15.80	0.0453	0.17
Palustrine Forested Wetland	30.00	30.00	0.09	0.15
Palustrine Scrub/Shrub Wetland	6.00	12.50	0.8589	0.07
Freshwater Marsh	0.76	0.56	578	0.07
Intermediate Marsh	0.50	0.20	2095	0.06
Estuarine Scrub/Shrub Wetland	1.98	6.90	0.66	0.07
Brackish Marsh	0.50	0.15	740	0.06
Saline Marsh	0.40	0.37	341	0.035

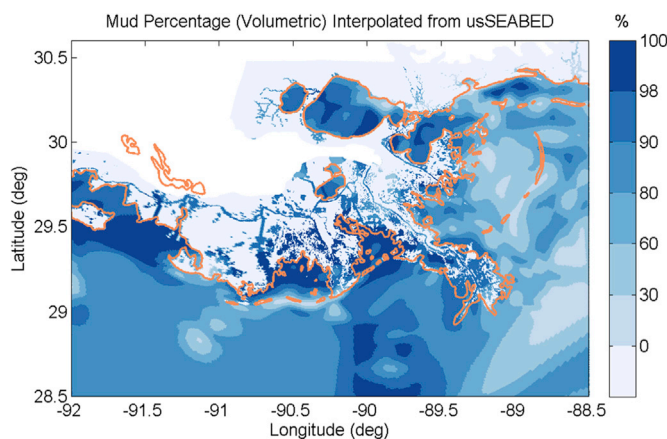


**Fig. 5.** The initial bed mud fraction interpolated from usSEABED (Williams et al., 2006).

elevation model (DEM) output from the wetland and barrier shoreline morphology models (Couvillion et al., 2013; Hughes et al., 2012) and LIDAR data from the national elevation dataset (NED, <http://nationalmap.gov/elevation.html>) were further applied for marshes and bayous in the Breton Sound estuary, Barataria Bay and Terrebonne Bay.

**2.3.2. Wind and waves**

An improved parametric wind model for asymmetric hurricanes (Hu et al., 2012) was used to simulate the wind field and air pressure during Hurricane Gustav. Storm parameters were obtained from the National

**Table 2**

The median diameter (D<sub>50</sub>) of sand, the settling velocity (ω<sub>s</sub>), critical shear stress (τ<sub>crit</sub>) and erosion rate (E) of mud in multiple studies.

Literature	Study site	Models	D <sub>50</sub> (mm)	Settling velocity (mm/s)	Critical shear stress (Pa)	Erosion rate (10 <sup>-4</sup> kg/m <sup>2</sup> /s)
Edmonds and Slingerland (2009)	Atchafalaya Bay	Delft3D	0.125, 0.225, 0.350	/	0.1–2.0	/
Leadon (2015)	Barrier Islands within Barataria	SBEACH	0.10–0.15	/	/	/
Nardin and Edmonds (2014)	Wax Lake Delta	Delft3D	0.10	/	0.25	/
Xu et al. (2011)	Texas-LA Continental shelf	ROMS	/	0.1, 1.0	0.03, 0.11	0.5
Xu et al. (2015)	Texas-LA Continental shelf	ROMS	0.063, 0.250	0.1, 1.0	0.11, 0.13	2.0, 3.0
Freeman et al. (2015)	Sister Lake	MIKE 21/3	/	/	0.15	/
Wright et al. (1997)	continental shelf to the south of Terrebonne Bay	*	/	/	0.1	/

Hurricane Center (NHC)'s best track data (<http://www.nhc.noaa.gov/data/>). The large-scale background wind provided by the National Center for Environmental Prediction (NCEP) was merged with the hurricane winds. Comparisons of wind speed/wind direction with measurements at twelve stations were given by Hu et al. (2012). They found the root-mean-square error (RMSE) of wind speed at all stations was 2.6 m/s with a correlation coefficient (R-squared) of 0.92.

The effects of surface waves and wave-current interactions were included by coupling the storm surge model with the third-generation spectral wave model SWAN (Booij et al., 1999). The wave calculation was performed every 60 min and the exchange of information between the wave model and the storm surge model took place at the same interval. The 60 min time step was chosen as a compromise between computational efficiency and accuracy.

**2.3.3. Vegetation effects**

Vegetation plays a unique role in coastal protection by attenuating strong winds, waves and storm surge. In our model, the flow resistance caused by vegetation drag was modeled as a drag force in the momentum equation, and it was strictly separated from the bed friction itself (without vegetation) to avoid unrealistic exaggeration of bed shear stress for sediment transport (Baptist, 2005). The spatial distribution of vegetation types was determined according to a coastal-wide aerial survey by USGS in 2007 (Sasser et al., 2008). Eleven vegetation types were included in the model (Table 1). The corresponding physical properties, namely vegetation height, stem diameter and vegetation density, were specified based on USDA Natural Resources Conservation (NRCS) herbaceous plant online database (<http://plants.usda.gov/java/factSheet>) and other literature (Visser, 2007). The vegetation-enhanced Manning's value in the wave model was generated for each of the eleven vegetation types following the guidelines in (Dietrich et al., 2008).

The vegetation effects on wave height reduction were modeled by means of Madsen et al. (1988)'s formulation, where the roughness length was related to the local water depth *h* and vegetation-enhanced Manning's coefficient *n* in the following way:

$$z_0 = h \exp \left[ - \left( 1 + \frac{Kh^{\frac{1}{3}}}{n\sqrt{g}} \right) \right] \tag{1}$$

where *g* is the gravitational acceleration and *K* is the von Karman constant. At each SWAN time step, *z*<sub>0</sub> was updated using the computed water level from the storm surge model.

**2.3.4. Sediment parameters**

Two sediment types, mud and sand, were considered in our model. The initial composition of mud and sand on the bed was extracted from the usSEABED data (Williams et al., 2006). Over 47,000 historical surficial grain-size data points are available on the Texas-Louisianan shelf, most of which contain more than 80% of mud. These data were interpolated to generate the initial mud and sand fraction in the domain (Fig. 5). In some parameter settings, the erosion rate could be

**Table 3**  
A summary of sediment parameters used in the numerical experiments in this study.

		D <sub>50</sub> (mm)	Settling velocity (mm/ s)	Critical shear stress (Pa)	Erosion rate (10 <sup>-4</sup> kg/m <sup>2</sup> /s)
Sand		0.14	NA	NA	NA
Mud	Ocean	NA	0.1, 0.25, and 1.0	0.1	0.5, 1.0, and 5.0
	Estuary	NA	0.1, 0.25, and 1.0	0.1	0.5, 1.0, and 5.0
	Wetland	NA	0.1, 0.25, and 1.0	1.0	0.5, 1.0, and 5.0

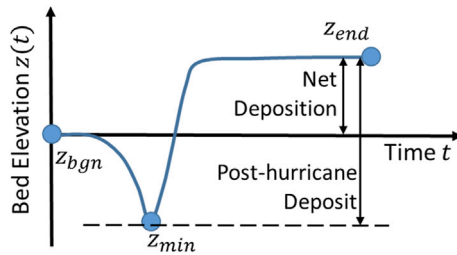


**Fig. 6.** The conceptual diagram of net deposition and post-hurricane deposit, modified after Xu et al (Xu et al., 2015). ( $z_{bgn}/z_{end}$ : the bed elevation at the beginning/end of the hurricane event;  $z_{min}$ : the minimum bed level ever experienced during the hurricane).

overestimated and the sediment supply at the bottom of the water body could be exhausted during the simulation if the initial sediment thickness is not large enough. Therefore, an initial sediment layer of 5 m was assumed in the model to prevent the removal of the “sediment reservoir” in sensitivity tests (details in section 4.1.). To track the source of sediment deposition, we further divide the sediment according to their initial location, i.e. whether it is located on the continental shelf, in the estuaries or on the wetlands at the beginning of the simulations, and it ends up with six different sediment groups in the simulations: mud from sea, mud from bay, mud from wetland, sand from sea, sand from bay, and sand from wetland.

The Partheniades-Krone approach (Partheniades, 1965) was used to model the erosion and deposition of mud on the bed. The method in (van Rijn, 2001) was chosen to account for erosion and deposition of sand. Several sediment properties are important in simulating erosional and depositional processes in the model: the median diameter ( $D_{50}$ ) of sand, the settling velocity ( $\omega_s$ ), critical shear stress ( $\tau_{crit}$ ) and erosion rate ( $E$ ) of mud. To determine a reasonable range of these parameters, we did a literature search on numerical simulations of sediment transport in coastal Louisiana (Table 2). Based on the literature, the median diameter of sand was set to 0.14 mm according to a study on barrier islands in the Barataria Basin (Leadon, 2015). For mud, we chose three settling velocities at 0.1, 0.25, and 1.0 mm/s and three erosion rates at 0.5, 1.0, and  $5.0 \times 10^{-4} \text{ kg m}^{-2} \text{ s}^{-1}$ , comparable to the values used in past studies. The critical shear stress was 0.1 Pa for mud on the shelf and in coastal bays, which was consistent with other numerical studies in the same region (Freeman et al., 2015; Xu et al., 2015). On the vegetated wetland surface, the critical shear stress was set to 1.0 Pa to account for the fact that vegetation roots can strengthen the soil layer and enhance its resistance to erosion. The sediment density was  $2650 \text{ kg/m}^3$  for sand and  $1600 \text{ kg/m}^3$  for mud. The sediment properties used in the experiments in this study were summarized in Table 3. The sediment concentration in the water column was assumed to be zero at the beginning of the simulation. Neumann-type boundary conditions were imposed for both mud and sand at the open boundary.

The sediment transport model for Hurricane Gustav was coupled with the simulation of hurricane wind, storm surge and waves. The detailed data flow in the coupled model were described in (Liu et al., 2015).

## 2.4. Model validation

Measurement data including water levels, waves and sediment depositions were used for model validation. To quantify the agreement between the modeled and the observed hydrodynamic processes, the normalized bias and the Scatter Index (SI) (Dietrich et al., 2008) of the time series were defined as the following:

$$\text{Bias} = \frac{\frac{1}{N} \sum_{i=1}^N E_i}{\frac{1}{N} \sum_{i=1}^N |O_i|} \quad (2)$$

and

$$\text{SI} = \frac{\sqrt{\frac{1}{N} \sum_{i=1}^N (E_i - \bar{E})^2}}{\frac{1}{N} \sum_{i=1}^N |O_i|} \quad (3)$$

where  $N$  is the number of observation points in the time series,  $E_i = S_i - O_i$  is the difference between the model result  $S_i$  and the observation  $O_i$ . By definition, bias describes the normalized mean error. **SI**, the standard deviation of  $E_i$ , indicates how much the predicted variation pattern deviates from the observed one. A smaller **SI** means more similarity between the simulated and the observed time series.

To validate model predictions of sediment transport, predicted post-hurricane deposit in wetlands was compared to measurements in Tweel and Turner (2012). As pointed out by Xu et al. (2015), two types of “deposition” should be distinguished: the “net deposition”

$$DEP_n = z_{end} - z_{bgn} \quad (4)$$

is the arithmetical difference between the bed elevation after and before the hurricane; and the “post-hurricane deposit”.

$$DEP_p = z_{end} - z_{min} \quad (5)$$

is the amount of deposition above the deepest cut ( $z_{min}$  in Fig. 6). Net deposition is not necessarily the same as post-hurricane deposit as illustrated in Fig. 6. Since Tweel and Turner (2012) measured the thickness of a fresh event layer without records of pre-hurricane elevation, it is the post-hurricane deposit, instead of the net deposition, from the model that corresponds to the measurements.

We also noticed large variations in the observed accretion even at locations very close to each other. This is not surprising given the fact that marsh surface topography can be complex with local features. In our model, mesh resolution was limited and not sufficient to resolve the small-scale features such as creeks and small ponds. Therefore, instead of a point-by-point comparison, the mean accretion at the measured sites within Terrebonne Bay and Barataria Bay (the division of basins was plotted in Fig. 1) and the standard errors were computed and validated against the corresponding mean value from field measurement.

In addition, experimental runs with varying sediment parameters were carried out to determine the “optimal” parameters. For each combination of different values of settling velocity, erosion rate and critical shear stress, we evaluated the overall error as the following

$$\delta = \frac{\delta_B n_B + \delta_T n_T}{n_B + n_T} \quad (6)$$

where  $\delta_B/\delta_T$  are the absolute error of mean accretion and  $n_B/n_T$  are the number of data points for Barataria Bay and Terrebonne Bay, respectively. The parameters corresponding to the minimum overall error were considered as the optimal ones.

## 2.5. Sediment flux analysis

To evaluate sediment exchange within the system from continental shelf to estuaries and wetlands, four cross sections were defined around

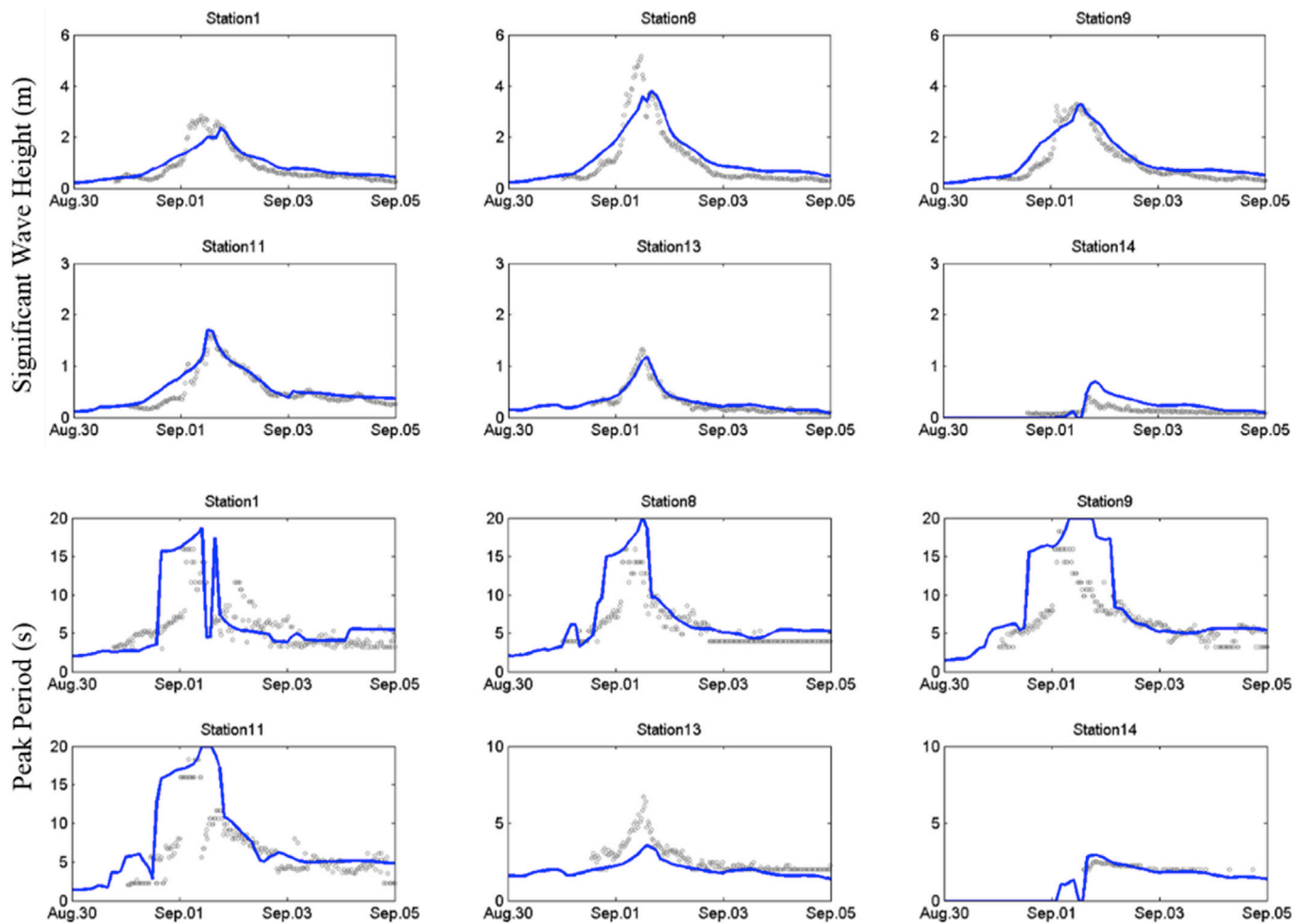


Fig. 7. Comparison of modeled wave heights and periods (blue lines) with the observations (grey circles) in Kennedy et al. (2010). (For interpretation of the references to color in this figure legend, the reader is referred to the Web version of this article.)

Barataria Bay (B1, B2) and Terrebonne Bay (T1, T2) (Fig. 1). B1 and T1 were located between the continental shelf and the coastal bays, while B2 and T2 were between estuaries and coastal wetlands (Fig. 1).

The sediment flux for each of the six sediment groups (mud from sea/bay/wetland and sand from sea/bay/wetland) was evaluated at these four cross sections. To be specific, we defined the total transport  $T_i(t)$  of the  $i$ -th sediment group at one of the cross sections B1/B2/T1/T2 to be

$$T_i(t) = \int_L S_i(x, y; t) dl \quad (7)$$

where  $S_i(x, y; t)$  is the total sediment transport per unit length per unit time ( $m^2/s$ ),  $L$  is the length of one of the four cross sections (m), and  $i = 1, \dots, 6$  for the six sediment groups.  $T_i$  and  $S_i$  are positive when the flux is from the continental shelf to the estuaries or from the estuaries to inland.

The time integration of  $T_i(t)$  over the hurricane event (from  $t_{bgn}$  to  $t_{end}$ ) gave the net onshore sediment transport  $M_i$  over each cross section, i.e.,

$$M_i = \int_{t_{bgn}}^{t_{end}} T_i(t) \rho_i dt \quad (8)$$

where  $\rho_i$  is the sediment density for each group.

To calculate the total deposition in wetlands ( $TDW$ ), we can evaluate

$$TDW = M_{mud,sea} + M_{mud,bay} \quad (9)$$

where  $M_{mud,bay}$  and  $M_{mud,sea}$  are mud material originating from coastal bays and sea, respectively. The percentage of sedimentation originating

from coastal bays (PB) to the total deposition on wetlands can be calculated as

$$PB = \frac{M_{mud,bay}}{M_{mud,bay} + M_{mud,sea}} \times 100\% \quad (10)$$

### 3. Results

#### 3.1. Hydrodynamic processes during Hurricane Gustav

The strong winds during Gustav generated large swells exceeding 10 m wave height to the southeast of the Louisiana coast. As the long waves approached the shoreline, they broke and dissipated quickly due to the shallow continental shelf and the bottom friction. At nearshore wave station 1, 8, and 9 (Kennedy et al., 2010) outside of Terrebonne Bay, where the local water depth was 7–10 m, the maximum significant wave heights were 3–5 m, while at station 11 in the southeast corner of Barataria Bay, the local water depth was 3.5 m and the peak significant wave height was less than 2 m (Fig. 7). We notice there was a significant underestimate of wave height at Station 8, which may be due to the uncertainty of the modeled hurricane wind field near the eye wall. Fig. 2 shows that Gustav passed right through Station 8, and we know that wind field changes dramatically near the hurricane center. Therefore, any errors in the hurricane track (location and/or timing) and the wind field cause large errors in the modeled waves at Station 8. The peak periods at all these stations were between 15 and 20 s. Stations 13 and 14 were located in the Caernarvon Marsh. The vegetation further attenuated wave

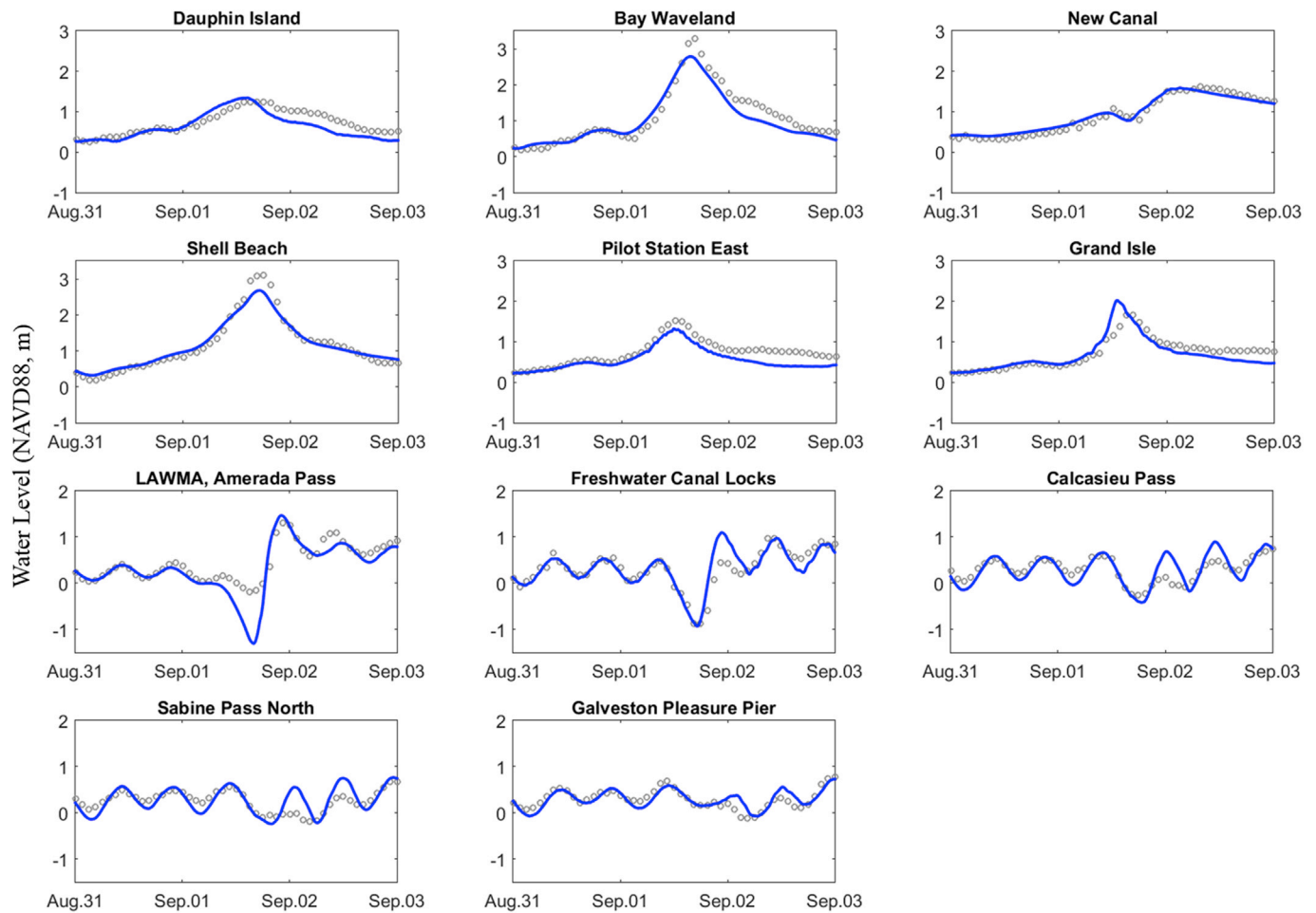


**Fig. 8.** Comparison of modeled water levels (blue lines) with observations (grey circles) at the NOAA tide stations. (For interpretation of the references to color in this figure legend, the reader is referred to the Web version of this article.)

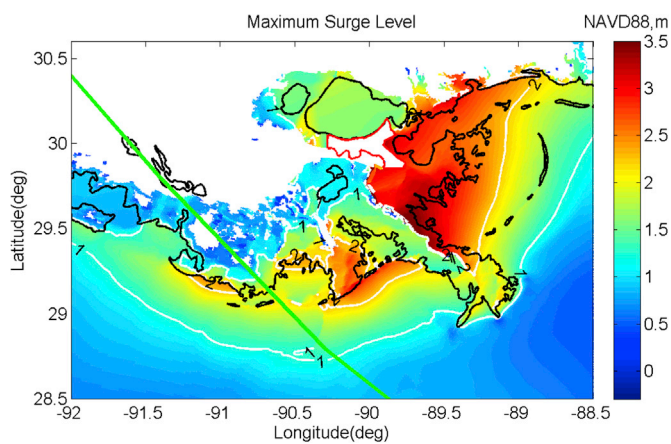


**Fig. 9.** Modeled maximum surge level in southeastern Louisiana during the passage of Gustav.

energy, and the wave height decreased with the inland distance. The wave model overestimated the wave height at Station 14, which may be explained by the limited spatial resolution of the biophysical properties of marsh vegetation and a lack of accurate representations of vegetation-induced energy dissipation. The peak period was underestimated at Station 13 by the model. Because the model resolution was not high enough to resolve the marsh surface, the inland Station 14 was

**Table 4**

The statistics for the agreement of wave and surge time series between measurements and model predictions.

	Variable	Number of stations	Bias	Scatter index
NOAA tide stations (southeastern LA)	Water Level (m)	6	-0.08	0.18
NOAA tide stations (total)	Water Level (m)	11	-0.06	0.35
Kennedy et al. (2010)	Water Level (m)	6	0.07	0.28
Kennedy et al. (2010)	Wave Height (m)	5	0.10	0.27
Kennedy et al. (2010)	Peak Wave Period (s)	6	0.17	0.41

excluded from the computation of model error and the resultant bias of wave height was 0.10. The bias of water level and peak periods for all the stations in Kennedy et al. (2010), were 0.07 and 0.17, respectively.

In general, the model prediction of storm surge was in good agreement with observations at NOAA tide stations (Fig. 8). In southeastern Louisiana, significant flooding can be observed and the highest storm surge appeared in the Breton Sound Basin (Fig. 9) owing to the long-lasting south-easterly wind and the blocking of the Mississippi River levee. Moreover, the peak surge occurred earlier in the area west of the Mississippi River than it did in the east. The bias and SI were -0.08 and 0.18 for the stations in this region (from Dauphin Island to Grand Isle). In the area west of the hurricane track, in contrast, the influence of storm

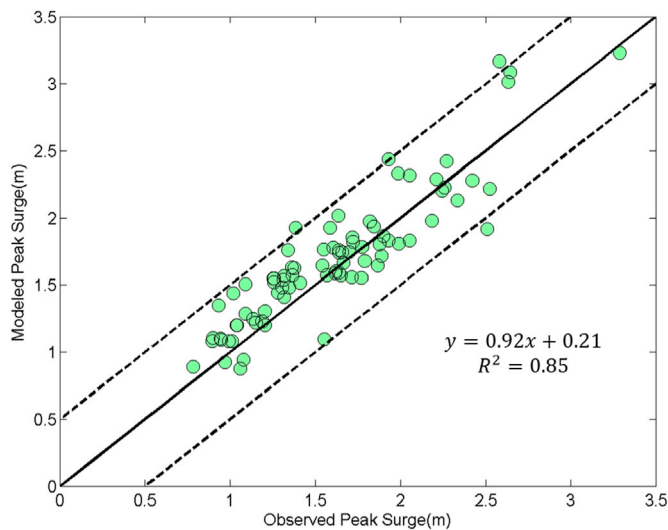


Fig. 10. Comparison of peak surges with the data records at the CRMS stations.

surge was rather limited, and model results captured the tidal variation of water level fairly well. Because of the relatively low water, the SI of all of the 11 stations was 0.35. The accuracy of model predictions of wave and surge time series is summarized in Table 4.

Accurately simulating the inland surge flooding is more challenging than that in the coastal water due to factors like vegetation-induced drag and local structures. To validate the model performance in predicting the extent of surge flooding in coastal wetlands, the modeled peak surge was compared with observations at the CRMS stations during Gustav (Fig. 10). The surge levels in Barataria Bay and Terrebonne Bay were in the range of 1–2 m. The slope and the R-squared of the best fit of peak surge at all the stations were 0.92 and 0.85, respectively. The good agreement between the modeled hydrodynamic forcing and the available field observations provides confidence for the modeling of hurricane-induced sediment transport and morphodynamics.

### 3.2. Hurricane-induced morphodynamics and post-hurricane accretion

The modeled wetland accretion and error statistics within each basin are presented in Table 5. The standard error of the mean accretion is the standard deviation of all the data samples divided by the square root of the sample size, and the overall error is defined by Equation (6). Among all the experimental runs, R11, R12, R22, R13 and R23 produced spatial-averaged accretion in the same order of magnitude as the field observation (Table 5). Because R12 has a minimum overall error  $\delta$  within the

numerical experiments, R12 with an erosion parameter of  $0.5 \times 10^{-4} \text{ kg m}^{-2} \text{ s}^{-1}$  and a settling velocity of 0.25 mm/s for mud was defined as the baseline model and the following discussion of model results were based on the settings in R12. Note that R12 may not be the only parameter combination which could generate a good match with the observation. But because the mean accretion rates within these three basins are very close to the field observations, we assume R12 is the “best-fit” solution and will discuss how the uncertainty in these parameters could affect our interpretation of the results and final conclusions in section 4.

A side-by-side comparison of simulated deposition with measurements in Tweel and Turner (2012) demonstrates the model not only produces a basin-averaged post-hurricane deposition close to the measurements, but also reveals that the net change of the sediment layer thickness at the selected survey locations could be considerably different from the fresh deposition measured after the hurricane (Fig. 11). For instance, the modeled net effect of Gustav was erosion at the survey sites in the Barataria Basin but the post-hurricane deposition was always positive by definition, suggesting the measured accretion was the deposit on the eroded wetland surface.

Three observation points (P01, P02 and P03 in Fig. 1) were selected in Terrebonne Bay to illustrate the evolution of hydrodynamic forcing and morphological changes. They represent three types of landscape characteristics: P01 was located in the open bay, P02 was in a small water pond, and P03 was initially on dry land. The maximum significant wave height decreased from 1.2 m in the shallow bay (P01) to 0.5 m on the marsh near the bay (P03) and the current also dropped from 1.5 m/s to 0.4 m/s due to the damping effect of vegetation. The modeled high shear stress was a combined result of strong currents and large waves during the hurricane (Fig. 12). In the shallow bay, an erosion of 8 cm was experienced prior to deposition (P01), which indicates a significant

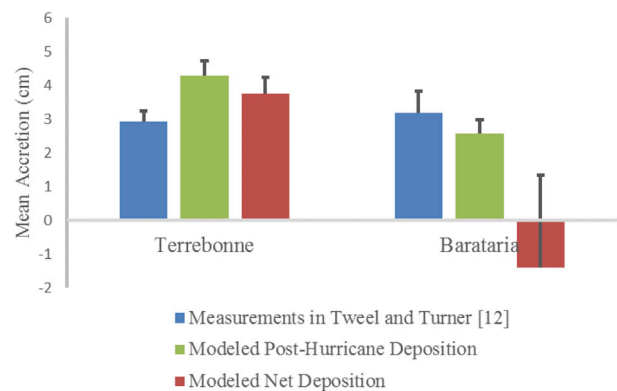


Fig. 11. Comparison of modeled deposition with measurements in Tweel and Turner, 2012.

Table 5

The sediment parameters used in numerical experiments and the mean accretion and standard error from each experimental run.

	Erosion rate ( $10^{-4} \text{ kg/m}^2/\text{s}$ )	Settling vel. (mm/s)	Critical shear stress: under water/vegetated land	Mean accretion (cm)		Standard error (cm)		Overall error (cm)
				Ter.	Bar.	Ter.	Bar.	
<i>Data from Tweel and Turner, 2012</i>								
				2.9	3.2	0.3	0.6	/
R11	0.5	0.1	0.1/1.0	6.6	3.6	0.6	0.4	2.2
R21	1.0	0.1	0.1/1.0	12.3	7.3	1.1	0.9	6.8
R31	5.0	0.1	0.1/1.0	46.1	28.2	4.5	4.1	33.8
R12	0.5	0.25	0.1/1.0	4.3	2.6	0.4	0.4	0.5
R22	1.0	0.25	0.1/1.0	8.3	5.3	0.8	0.8	3.8
R32	5.0	0.25	0.1/1.0	43.3	28.6	4.0	4.4	32.4
R13	0.5	1.0	0.1/1.0	1.2	0.9	0.2	0.2	-1.9
R23	1.0	1.0	0.1/1.0	2.5	1.8	0.4	0.5	-0.8
R33	5.0	1.0	0.1/1.0	12.2	13.4	1.7	2.8	9.2
X2	0.5	0.25	0.05/0.5	8.4	5.4	0.8	0.8	3.9
X3	0.5	0.25	0.2/2.0	2.1	1.3	0.2	0.2	-1.2

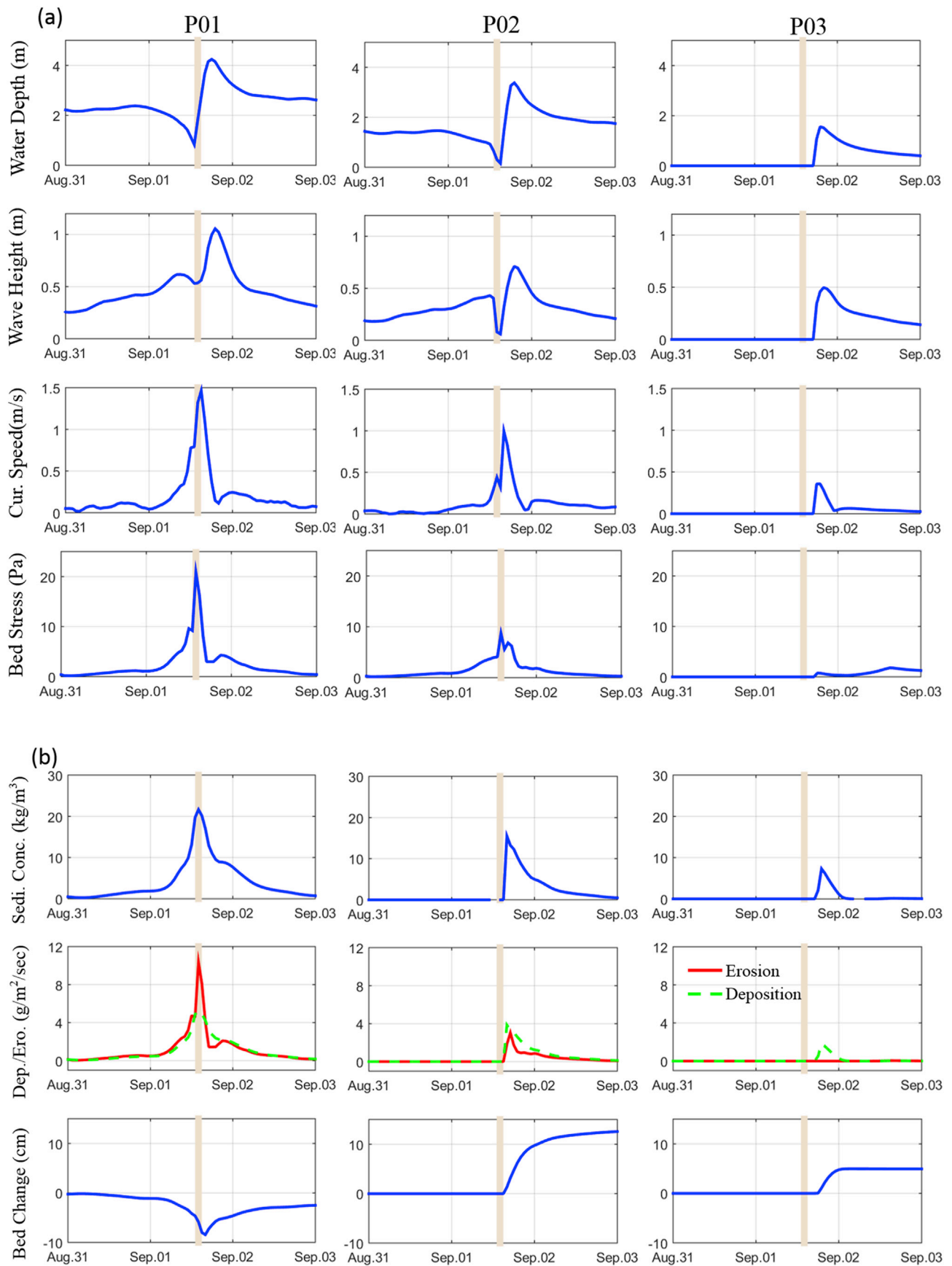
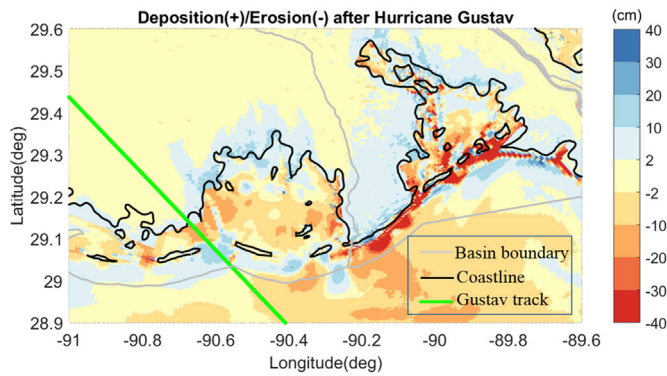


Fig. 12. Modeled hydrodynamics processes (a) and morphological processes (b) at P01/P02/P03 in Terrebonne Bay.



**Fig. 13.** The modeled net deposition/erosion (relative to the pre-storm bed sediment thickness) in the Terrebonne and Barataria Basins after Hurricane Gustav.

suspension in the open bay as the hurricane was approaching onshore. In the wetlands (P02 and P03), a direct deposition was more likely to happen for two reasons: first, the vegetation enhanced the soil strength and increased resistance to erosion; and secondly, the erosion was filled almost immediately by the deposition.

The net morphological change of the bed sediment layer after the hurricane is presented in Fig. 13. After Hurricane Gustav, the suspended sediment was widely spread into a large area of wetlands including the northern shore of Terrebonne Bay, the eastern shore of Barataria Bay and the wetlands between Terrebonne Bay and Barataria Bay, which agreed fairly well with the distribution of the deposition samples in Tweel and Turner (2012) (Fig. 3).

The morphological change is the results of the sediment redistribution in the wetlands-bay-continental shelf system under the hydrodynamic forcing. The total sediment transport, including all the six sediment groups (mud from sea, mud from bay, mud from wetland, sand from sea, sand from bay, and mud from wetland) during Hurricane Gustav, is presented in Fig. 14. At 4 h before landfall, the sediment transport was mainly in the easterly alongshore direction on the continental shelf due to the strong longshore current driven by the northeasterly winds in this area (Fig. 14 (a)). The largest transport rate, measured by the mass of transported sediment per unit time per unit cross section length, happened in the area close to the center of Gustav. After the landfall of Gustav, a strong onshore transport occurred in both Terrebonne Bay and Barataria Bay, and it lasted a few hours after Gustav's landfall (Fig. 14 (b) to (d)).

Compared with field studies on hurricane effects on coastal sediment transport, some unique characteristics of this numerical model are also worth mentioning. Firstly, our numerical model is capable of predicting the evolution of bed sediment layers during the hurricane event and distinguishing the two different types of sediment accumulation (illustrated in Figure 11 and Figure 12). This capability provides important complementary information to the field studies to evaluate the net morphological effects of the hurricane on the wetlands. Secondly, since field survey can only be carried out at a limited number of locations, a spatial-interpolation was often used to estimate the total deposition in coastal basins from the measured deposition at discrete locations (e.g., Tweel and Turner (2012) and Smith et al. (2015)). The underlying assumption of the interpolation is that deposition can be found everywhere in the basin, with the only difference in amount. But our model result reveals that at certain locations, the possible deposition could not balance the surface erosion, and the net effect of a hurricane is the loss of sediment surface layer (for instance, at point P01 in Fig. 1). Therefore, our simulations suggest that a simple interpolation of measured deposition over the whole basin may overestimate the net accretion amount caused by a hurricane because of the wetland fragmentation in coastal Louisiana.

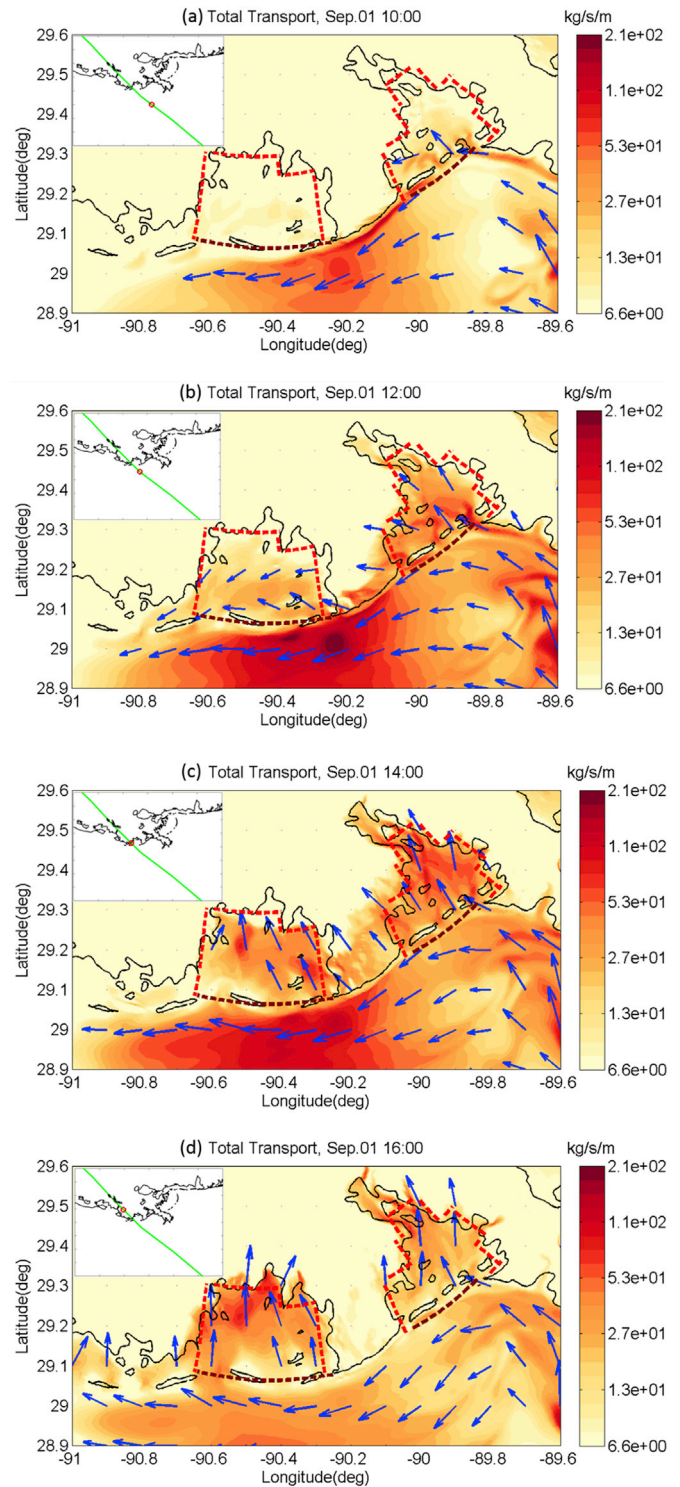


**Fig. 14.** The total sediment transport per unit time per unit cross section length at (a) 10:00 UTC (approximately 4 h before landfall), (b) 12:00 UTC (approximately 2 h before landfall), (c) 14:00 UTC (approximately landfall), and (d) 16:00 UTC (approximately 2 h after Gustav landfall) on 09/01/2008. The color contour shows the magnitude of the transport and the arrows show the direction of the transport. The red circles in the upper-left panel is the center of Hurricane Gustav at the same time. (For interpretation of the references to color in this figure legend, the reader is referred to the Web version of this article.)

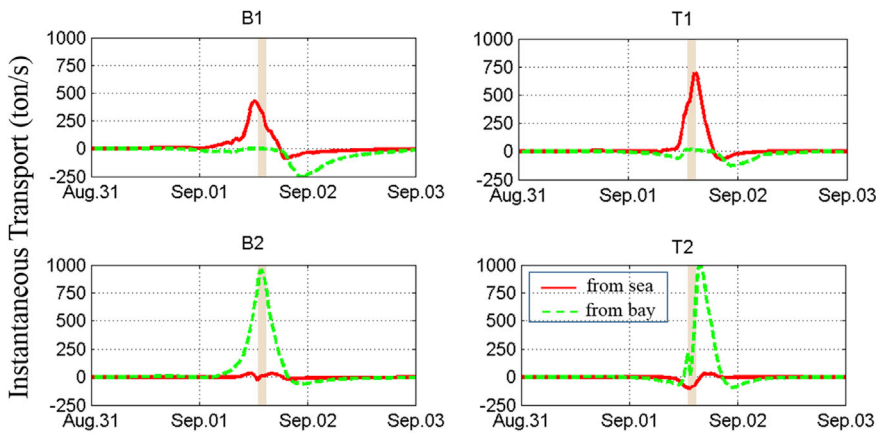


Fig. 15. The time series of the total suspended transport over the defined cross sections: from R12.

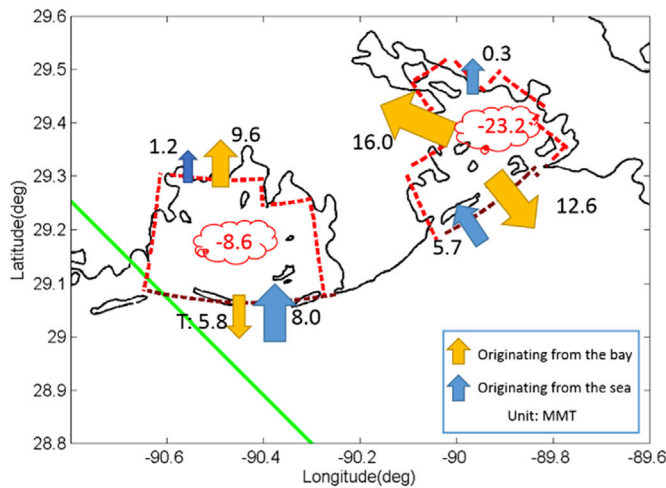


Fig. 16. The net sediment transport (in Million Metric Ton, MMT) over different cross sections in Terrebonne Bay and Barataria Bay during Hurricane Gustav.

### 3.3. Sediment fluxes and balance

Based on our numerical experiments, the suspension and transport of sand was much less than that of mud. Therefore, the redistribution of sediment under hurricane forcing mainly occurred to mud on the Louisiana coast. This finding is consistent with the measurements of post-hurricane deposition for Gustav and other hurricane events (Turner et al., 2006; Tweel and Turner, 2012; Freeman et al., 2015). In both Terrebonne Bay and Barataria Bay, we found a significant transport of marine material, from continental shelf to estuaries (cross section B1 and T1 in Fig. 15). At the cross sections between the estuaries and wetlands, however, sediment originating from the coastal estuaries dominated (cross section B2 and T2 in Fig. 15). As the soil on the vegetated wetland surface was harder to erode compared to mud flats, the contribution of sediments from vegetated wetlands was almost negligible compared with those from the ocean and the estuaries. We also noted that the peak of sediment transport appeared earlier in Barataria Bay than it did in Terrebonne Bay. This can be explained by the fact that the hurricane approached the coastline from a southeastern direction and the maximum wind and waves appeared earlier in the Barataria Basin.

Sediment fluxes at the cross-sections (Fig. 15) suggested that there were multiple processes going on during the hurricane: in-flux of sediment into the bay, suspension of muddy material from the bay bottom, and transport and redistribution of the suspended material. These processes were also noticed in the study of sediment transport in a typical

coastal Louisiana Lake (Sister Lake) by Freeman et al. (2015). If we consider the bounding box in Fig. 1 as an approximate boundary for Terrebonne Bay and Barataria Bay, we can calculate a sediment budget for each bay during the hurricane event (Fig. 16). Our model predicted that the amount of suspended fine sediment was much more than that transported into the bay from the Gulf of Mexico. The net erosion in Barataria Bay and Terrebonne Bay was 23.2 MMT and 8.6 MMT, respectively, during Hurricane Gustav. If we divide the net erosion by the surface area of Barataria Bay and Terrebonne Bay, the erosion was equivalent to a loss of mud layer with a thickness of 1.0 cm in Barataria and 0.3 cm in Terrebonne Bay, respectively.

The reasons why the amounts of erosion in these two bays were different could be twofold. The first reason is associated with the orientation of Barataria Bay relative to the wind direction of Gustav. As Gustav was moving towards the Louisiana Coast, the counter-clockwise wind field blew onshore and led to a significant surge in Barataria Bay while it was towards the offshore in Terrebonne Bay. Therefore, although Terrebonne Bay is closer to the hurricane track, the duration of the “disturbance” was shorter in Terrebonne Bay than that in Barataria Bay. The second reason is associated with the pattern of receding sediment flow. At the inlet of Barataria Bay, a long tail of sediment export occurred after the hurricane had passed (dashed line in B1, Fig. 15). A similar sediment export can be observed in Terrebonne Bay but with much smaller magnitude (dashed line in T1, Fig. 15). This difference may be attributed to the fact that the narrow and deep inlets of the barrier island chain in Barataria Bay served as an efficient pathway for sediment transport to the Gulf. The receding water flow at the narrow outlets was more energetic and carried more sediment back to the continental shelf compared with Terrebonne Bay. Due to the above reasons, the magnitude of sediment suspension and erosion in Terrebonne was smaller than that in Barataria during Gustav. Although the change of bed thickness was not large in either Barataria or Terrebonne, the long-term sediment balance of the coastal bays is worth further exploration.

## 4. Discussions

### 4.1. Model sensitivity to sediment parameters

The sensitivities of model results to settling velocity and erosion rate of mud are shown in Fig. 17. As settling velocity increased from 0.1 to 1.0 mm/s and erosion rate increased from 0.5 to 5.0  $\times 10^4$  kg/m<sup>2</sup>/s, the total deposition in the wetlands (TDW) varied by two orders of magnitude (from 1.8 to 177.3 MMT in Terrebonne Bay, and from 3.7 to 269.4 MMT in Barataria Bay). In general, with a larger erosion rate, more sediment can be suspended from the bed, and with less settling velocity, the suspended material is more likely to be transported far enough to reach the shoreline before it settles down again. Therefore, the largest TDW corresponded to the largest erosion rate and smallest settling

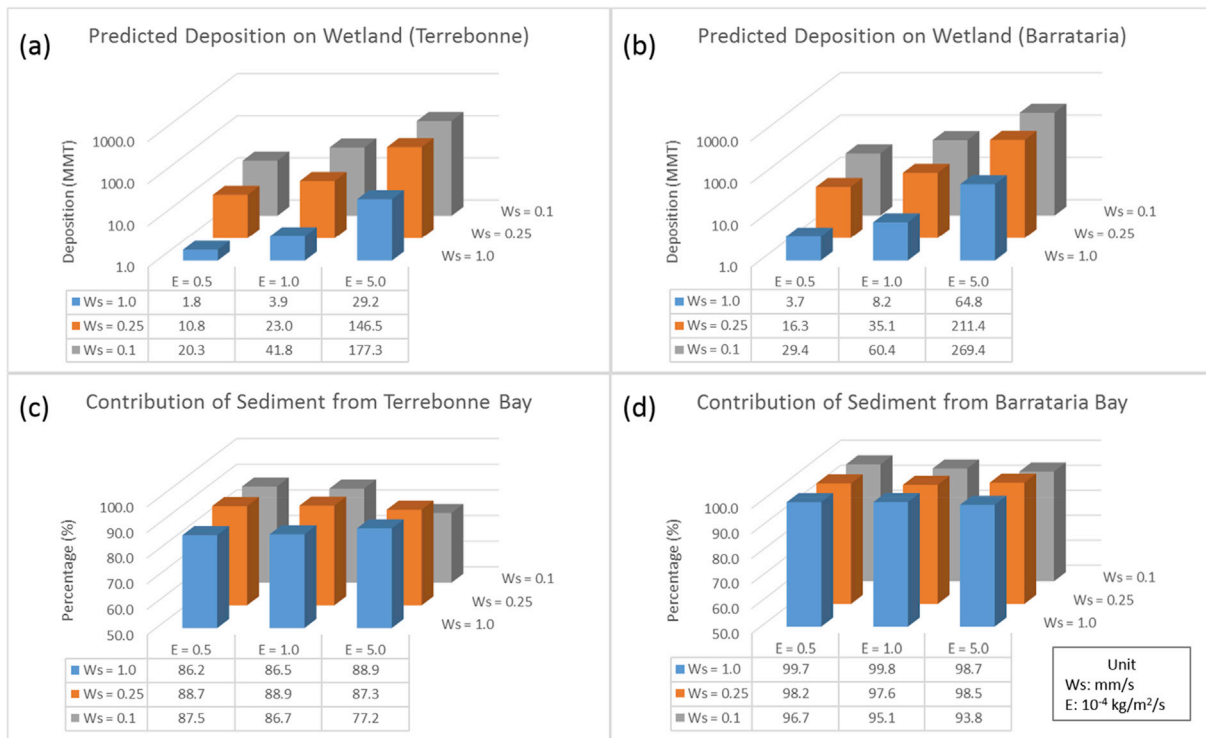


Fig. 17. Predicted total deposition on the wetland surface (a and b) and percentage of sediment from the coastal bays (c and d) with different settling velocity and erosion rate.

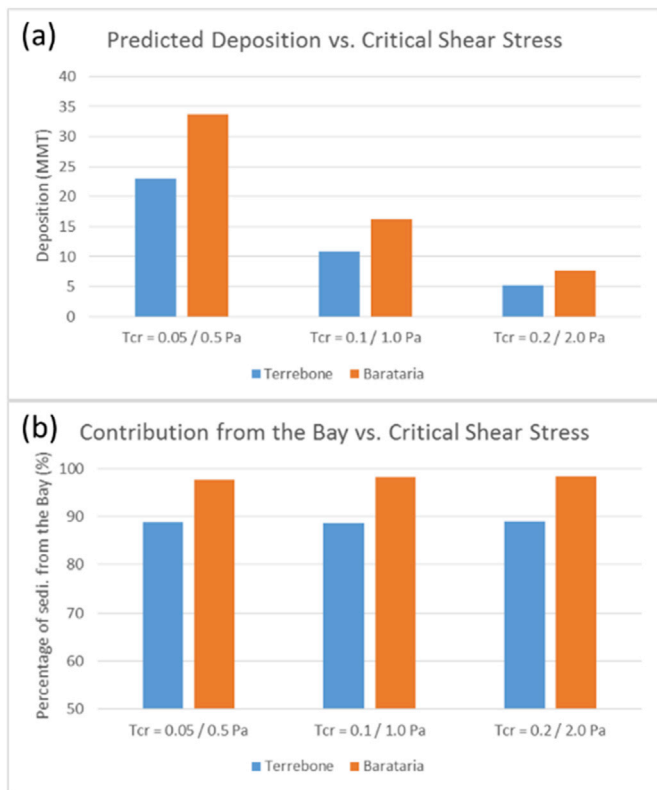


Fig. 18. Model sensitivity to critical shear stress.

velocity (Fig. 17 (a) and (b)). In contrast, in terms of the contributions of coastal bays to deposition in wetlands, the percentage of sedimentation originating from coastal bays (PB) seemed insensitive to these

parameters. The calculated PB for Terrebonne Bay and Barataria Bay was in the range of 77.2%–88.9% (with a mean of 86.4%) and 93.8%–99.8% (with a mean of 97.6%), respectively, regardless of the difference in settling velocity and erosion rate (Fig. 17 (c) and (d)).

Based on the baseline model (R12), numerical experiments were also conducted with different critical shear stress (X2 and X3 in Table 5). Similarly, the TDW decreased with critical shear stress for erosion, but the PB remained nearly constant within the range of critical shear stress in the experiments (Fig. 18). The above results indicate that the major source of wetland deposition being from the coastal bays is determined by the transport capability of nearshore circulation during the hurricane event.

#### 4.2. Uncertainty analysis

To analyze the relative contribution of each parameter to the total variance of results, the following dimensionless parameters were defined:

$$TDW' = \ln\left(\frac{TDW}{TDW_0}\right) \quad (11)$$

$$E' = \ln\left(\frac{E}{E_0}\right) \quad (12)$$

$$\omega'_s = \ln\left(\frac{\omega_s}{\omega_{s0}}\right) \quad (13)$$

$$\tau'_{crit} = \ln\left(\frac{\tau_{crit}}{\tau_{crit,0}}\right) \quad (14)$$

where  $TDW_0 = 27.1$  MMT,  $E_0 = 0.5 \times 10^4$  kg/m<sup>2</sup>/s,  $\omega_{s0} = 0.25$  mm/s,  $\tau_{crit,0} = 0.1$  Pa were given by the baseline run. Assuming the model prediction of TDW' can be approximated by a linearized response function of the dimensionless parameters  $E'$ ,  $\omega'_s$  and  $\tau'_{crit}$ , a multi-variate analysis gave the approximate sensitivity coefficient and variance associated with each

**Table 6**

The approximate sensitivity coefficient and the variance of each dimensionless sediment parameter.

Variable $X'$	Sensitivity coefficient	Standard deviation	The variance in $TDW'$ due to $X'$	Percentage (%)
$E'$	1.12	0.70	0.61	48.8
$\omega'_s$	-0.95	0.70	0.44	35.2
$\tau'_{crit}$	-1.06	0.42	0.20	16.0

sediment parameter (Table 6). The  $TDW'$  has a positive sensitivity coefficient with  $E'$  (1.12) and a negative sensitivity coefficient with  $\omega'_s$  (-0.95) and  $\tau'_{crit}$  (-1.06), which is consistent with our observations in Fig. 17 and Fig. 18.

The effect of uncertainties of these three parameters on the modeled deposition in wetlands can be measured by the percentage of each parameter's contribution to the total variance in the  $TDW'$ . The variance in the erosion rate  $E'$  accounts for 48.8% of the variance in the  $TDW'$ , while only 35.2% and 16.0% of the total variance were represented by the settling velocity  $\omega'_s$  and critical shear stress  $\tau'_{crit}$ . In other words, most of the uncertainty in the  $TDW'$  was caused by the uncertainty in the erosion rate. Assuming the uncertainty in  $TDW'$  follows a Gaussian distribution around the baseline run, the 5 to 95 percentile interval for the predicted deposition on wetland surface was [4.3, 170.0] MMT.

In reality, critical shear stress could vary in space and time, and settling velocity and erosion rate are also variables depending on sediment properties and flow conditions. But in this paper they are simplified to be constants in time and a uniform value for sediment under water and on the vegetated wetlands, respectively. The scarcity of data for these parameters highlights the need for a more detailed sediment dataset on the Louisiana coast.

Another limitation is that the sediment transport due to the overwash and possible breaching of barrier islands during Hurricane Gustav was not considered in this study. Although this omission does not affect the conclusions of the study because the area of both estuaries is much greater than the area of the barrier islands and no significant breaching occurred during Hurricane Gustav, coupling XBEACH with Delft3D to quantify the sediment transport associated with overwash and barrier island degradation is of interest and worth pursuing in the future.

## 5. Conclusions

The understanding of hurricane-induced sedimentation in coastal wetlands has been expanded through a coupled hurricane wind, storm surge, wave and sediment transport modeling system in the present study. This model successfully reproduced the observed hydrodynamic response in the coastal zone during Hurricane Gustav (2008), and the modeled storm surge and waves were validated extensively with field observations along the coast. The simulations showed that during a hurricane event, the sediment suspension and redistribution mainly occurred to mud on the mud-dominant Louisiana coast; in contrast, the transport of sand was relatively negligible during the hurricane. The modeled spatial range and mean sediment accretion on the vegetated wetland surface within the Terrebonne and Barataria Basins were in good agreement with the measurements of fresh deposition after Gustav by Tweel and Turner (2012).

The model prediction of wetland deposition in the Terrebonne and Barataria Basins during Gustav was sensitive to some sediment properties in the model, i.e., settling velocity, erosion rate and critical shear stress. Among them, uncertainty in erosion rate constituted the major part of the variance in the predicted deposition. Based on a baseline setting verified by the basin-average sediment accretion, the sediment deposition in coastal wetlands during Gustav was about 27 MMT, and the 5 and 95 percentile interval was [4.3, 170.0] MMT.

The long-existing hypothesis about the source of deposition in

wetlands during a hurricane was verified via numerical simulation for the first time. Our model results indicate that the suspended material from the coastal bays made up 88.7% of wetland deposition in Terrebonne Bay and 98.2% in Barataria Bay during Hurricane Gustav. During the large-scale (but short-term) sediment transport and redistribution, Terrebonne Bay and Barataria Bay acted as a major source of sediment transported to the adjacent coastal wetlands. The implication of the present study for coastal restoration in south Louisiana is that keeping sediments from the Mississippi River within the estuaries is essential.

## Acknowledgments

The study was supported in part by the National Science Foundation (SEES-1427389, and CCF-1539567) and the Louisiana Sea Grant. Dr. R. Eugene Turner provided the wetland sedimentation data. Drs. Chunyan Li and Justic Dubravko provided the bathymetric data of Barataria Bay. Dr. Haihong Zhao and Ms. Lixia Wang provided the LIDAR data in Barataria Bay and Terrebonne Bay. Mr. Brady Covillion and Dr. Hongqing Wang provided the vegetation distribution data. Haikuo Yu provided assistance in processing GIS data. Computational resources were provided by Louisiana Optical Network Initiative (LONI) and LSU High Performance Computing.

## References

- Baptist, M.J., 2005. *Modelling Floodplain Biogeomorphology*. ISBN 90-407-2582-9.
- Booij, N., Ris, R.R.C., Holthuijsen, L.H.L., 1999. A third-generation wave model for coastal regions I. Model description and validation. *J. Geophys. Res.* 104, 7649–7666. <https://doi.org/10.1029/98jc02622>.
- Cahoon, D.R., Reed, D.J., Day, J., Teyer, J.W.G.D., Boumans, R.M., Lynch, J.C., McNally, D., Latif, N., 1995. The influence of Hurricane Andrew on sediment distribution in Louisiana coastal marshes. *J. Coast. Res. Sp. Issue* 280–294. <http://www.jstor.org/stable/10.2307/25736015>.
- Chamberlain, J.L., 1959. *Influence of Hurricane Audrey on the Coastal Marsh of Southwestern Louisiana*. Technical Report No. 10, Part B, Baton Rouge.
- Chen, Q., Wang, L., Tawes, R., 2008. Hydrodynamic response of northeastern Gulf of Mexico to hurricanes. *Estuar. Coast* 31, 1098–1116. <https://doi.org/10.1007/s12237-008-9089-9>.
- Couvillion, B.R., Barras, J.A., Steyer, G.D., Sleavin, W., Fischer, M., Beck, H., Trahan, N., Griffin, B., Heckman, D., 2011. Land Area Change in Coastal Louisiana from 1932 to 2010.
- Couvillion, B.R., Steyer, G.D., Wang, H., Beck, H.J., Rybczyk, J.M., 2013. Forecasting the effects of coastal protection and restoration projects on wetland morphology in coastal Louisiana under multiple environmental uncertainty scenarios. *J. Coastline Res.* 29–50.
- Dietrich, J.C., Westerink, J.J., Kennedy, a. B., Smith, J.M., Jensen, R.E., Zijlema, M., Holthuijsen, L.H., Dawson, C., Luettich, R. a., Powell, M.D., Cardone, V.J., Cox, a. T., Stone, G.W., Pourtaheri, H., Hope, M.E., Tanaka, S., Westerink, L.G., Westerink, H.J., Cobell, Z., Hurricane Gustav, 2008. Waves and storm surge: Hindcast, synoptic analysis, and validation in southern Louisiana. *Mon. Weather Rev.* 139 (2011), 2488–2522. <https://doi.org/10.1175/2011MWR3611.1>.
- Edmonds, D.A., Slingerland, R.L., 2009. Significant effect of sediment cohesion on delta morphology. *Nat. Geosci.* 3, 105–109. <https://doi.org/10.1038/ngeo730>.
- Freeman, A.M., Jose, F., Roberts, H.H., Stone, G.W., 2015. Storm induced hydrodynamics and sediment transport in a coastal Louisiana lake. *Estuar. Coast Shelf Sci.* 161, 65–75. <https://doi.org/10.1016/j.ecss.2015.04.011>.
- Horstman, E.M., Dohmen-Janssen, C.M., Hulscher, S., 2013. Modeling tidal dynamics in a mangrove creek catchment in Delft3D. In: *Proc. Coast. Sediments*, vol. 2013, pp. 833–844.
- Horstman, E.M., Dohmen-Janssen, C.M., Bouma, T.J., Hulscher, S.J.M.H., 2015. Tidal-scale flow routing and sedimentation in mangrove forests: combining field data and numerical modelling. *Geomorphology* 228, 244–262. <https://doi.org/10.1016/j.geomorph.2014.08.011>.
- Hu, K., Chen, Q., Kimball, S.K., 2012. Consistency in hurricane surface wind forecasting: an improved parametric model. *Nat. Hazards* 61, 1029–1050.
- Hu, K., Chen, Q., Wang, H., 2015. A numerical study of vegetation impact on reducing storm surge by wetlands in a semi-enclosed estuary. *Coast. Eng.* 95, 66–76. <https://doi.org/10.1016/j.coastaleng.2014.09.008>.
- Hughes, Z., Weathers, D., Georgiou, I., FitzGerald, D., Kulp, M., 2012. *Barrier island morphology model technical report (Appendix D-3)*. In: *Louisiana's comprehensive master plan for a sustainable coast*. Louisiana.
- Kennedy, A.B., Gravois, U., Zachry, B., Luettich, R., Whipple, T., Weaver, R., Reynolds-Fleming, J., Chen, Q.J., Avissar, R., 2010. Rapidly installed temporary gauging for hurricane waves and surge, and application to Hurricane Gustav. *Cont. Shelf Res.* 30, 1743–1752. <https://doi.org/10.1016/j.csr.2010.07.013>.
- Lapetina, A., Sheng, Y.P., 2015. Simulating complex storm surge dynamics: three-dimensionality, vegetation effect, and onshore sediment transport. *J. Geophys. Res. Ocean* 120, 7363–7380.

- Leadon, M., 2015. Beach slope and sediment-grain-size trends as a basis for input parameters for the SBEACH erosion model. *J. Coast Res.* 31, 1375–1388.
- Liu, K., Chen, Q., Hu, K., Xu, K., 2015. Numerical simulation of sediment deposition and erosion on Louisiana coast during Hurricane Gustav. In: *Proc. Coast. Sediments*, vol. 2015.
- Madsen, O.S., Poon, Y.K., Graber, H.C., 1988. Spectral wave attenuation by bottom friction. *Theory, Coast. Eng.* 492–504. <https://doi.org/10.9753/icce.v21>.
- McGee, B.D., Goree, B.B., Tollett, R.W., Woodward, B.K., Kress, W.H., 2006. Hurricane Rita Surge Data, Southwestern Louisiana and Southeastern Texas, September to November 2005.
- McKee, K.L., Cherry, J.A., 2009. Hurricane Katrina sediment slowed elevation loss in subsiding brackish marshes of the Mississippi River delta. *Wetlands* 29, 2–15.
- Morgan, J.P., Nichols, L.G., Wright, M., 1958. Morphological Effects of Hurricane Audrey on the Louisiana Coast, Baton Rouge.
- Morton, R.A., Barras, J.A., 2011. Hurricane impacts on coastal wetlands: a half-century record of storm-generated features from southern Louisiana. *J. Coast Res.* 27, 27–43.
- Nardin, W., Edmonds, D.A., 2014. Optimum vegetation height and density for inorganic sedimentation in deltaic marshes. *Nat. Geosci.* 7, 722–726. <https://doi.org/10.1038/ngeo2233>.
- Nyman, J.A., Crozier, C.R., DeLaune, R.D., 1995. Roles and patterns of hurricane sedimentation in an estuarine marsh landscape. *Estuar. Coast Shelf Sci.* 40, 665–679. <https://doi.org/10.1006/ecss.1995.0045>.
- Partheniades, E., 1965. Erosion and deposition of cohesive soils. *J. Hydraul. Div.* 91, 105–139.
- Reed, D.J., 1989. Patterns of sediment deposition in subsiding coastal salt marshes, Terrebonne Bay, Louisiana: the role of winter storms. *Estuaries* 12, 222–227. <https://doi.org/10.1007/BF02689700>.
- Rejmánek, M., Sasser, C.E., Peterson, G.W., 1988. Hurricane-induced sediment deposition in a gulf coast marsh. *Estuar. Coast Shelf Sci.* 27, 217–222. [https://doi.org/10.1016/0272-7714\(88\)90091-1](https://doi.org/10.1016/0272-7714(88)90091-1).
- Roberts, H., Huh, O., Hsu, S., Rouse, L., Rickman, D., 1987. Impact of cold-front passages on geomorphic evolution and sediment dynamics of the complex Louisiana coast. In: *Coast. Sediment*, pp. 1950–1963.
- Sasser, C.E., Visser, J.M., Mouton, E., Linscombe, J., Hartley, S.B., 2008. Vegetation Types in Coastal Louisiana in 2007. U.S. Geological Survey Open-File Report 2008-1224. <http://pubs.usgs.gov/of/2008/1224/>.
- Smith, J.E., Bentley, S.J., Snedden, G.A., White, C., 2015. What role do hurricanes play in sediment delivery to subsiding river deltas? *Sci. Rep.* 5, 17582. <https://doi.org/10.1038/srep17582>.
- Turner, R.E., Baustian, J.J., Swenson, E.M., Spicer, J.S., 2006. Wetland sedimentation from hurricanes Katrina and Rita. *Science* (80-) 314, 449–452. <https://doi.org/10.1126/science.1129116>.
- Tweel, A.W., Turner, R.E., 2012. Landscape-scale analysis of wetland sediment deposition from four tropical cyclone events. *Plos One* 7. <https://doi.org/10.1371/journal.pone.0050528>.
- van Rijn, L.C., 2001. General View on Sand Transport by Currents and Waves: Data analysis and engineering modelling for uniform and graded sand (TRANSPOR 2000 and CROSMOR 2000 models). Z2899.20/Z2099.30/Z2824.30., Delft.
- Visser, J.M., 2007. Hydrologic Characteristics of Louisiana's Coastal Eetland Vegetation. Literature Summary for URS Group, Inc.. Louisiana State University, Baton Rouge, LA.
- Wang, H., Chen, Q., Hu, K., Snedden, G.A., Hartig, E.K., Couvillion, B.R., Johnson, C.L., Orton, P.M., 2017. Numerical Modeling of the Effects of Hurricane Sandy and Potential Future Hurricanes on Spatial Patterns of Salt Marsh Morphology in Jamaica Bay, New York City. U.S. Geological Survey Open-File Report 2017–1016. <https://doi.org/10.3133/ofr20171016>.
- Warner, J.C., Schwab, W.C., List, J.H., Safak, I., Liste, M., Baldwin, W., 2017. Inner-shelf ocean dynamics and seafloor morphologic changes during Hurricane Sandy. *Cont. Shelf Res.* 138, 1–18.
- Williams, S.J., Arsenault, M.A., Buczkowski, B.J., Reid, J.A., Flocks, J.G., Kulp, M.A., Penland, S., Jenkins, C.J., 2006. Surficial Sediment Character of the Louisiana Offshore Continental Shelf Region: A GIS Compilation. U.S. Geological Survey Open-File Report 2006-1195.
- Wright, L.D., Sherwood, C.R., Sternberg, R.W., 1997. Field measurements of fairweather bottom boundary layer processes and sediment suspension on the Louisiana inner continental shelf. *Mar. Geol.* 140, 329–345. [https://doi.org/10.1016/S0025-3227\(97\)00032-7](https://doi.org/10.1016/S0025-3227(97)00032-7).
- Xu, K., Harris, C.K., Hetland, R.D., Kaihatu, J.M., 2011. Dispersal of Mississippi and Atchafalaya sediment on the Texas-Louisiana shelf: model estimates for the year 1993. *Cont. Shelf Res.* 31, 1558–1575. <https://doi.org/10.1016/j.csr.2011.05.008>.
- Xu, K., Mickey, R.C., Chen, Q., Harris, C.K., Hetland, R.D., Hu, K., Wang, J., 2015. Shelf sediment transport during hurricanes Katrina and Rita. *Comput. Geosci.* 1–16. <https://doi.org/10.1016/j.cageo.2015.10.009>.
- Yamashita, K., Sugawara, D., Takahashi, T., Imamura, F., Saito, Y., Imato, Y., Kai, T., Uehara, D., 2016. Numerical simulations of large-scale sediment transport caused by the 2011 tohoku earthquake tsunami. In: *Hirota Bay, Southern Sanriku Coast, Coast. Eng. J.*, vol. 58. <https://doi.org/10.1142/S0578563416400155>.